TERM ● CrossMark

ORIGINAL ARTICLE

Effect of Drug Carrier Melting Points on Drug Release of Dexamethasone-Loaded Microspheres

Ji Hoon Park[1] · Doo Yeon Kwon[1] · Ji Yeon Heo[1] · Seung Hun Park[1] ·
Joon Yeong Park[1] · Bong Lee[2] · Jae Ho Kim[1] · Moon Suk Kim[1]

Abstract Here, we examined the effect of melting point of drug carriers on drug release of dexamethasone (Dex)-loaded microspheres. We prepared poly(L-lactide-ran-ε-caprolactone) (PLC) copolymers with varying compositions of poly(ε-caprolactone) (PCL) and poly(L-lactide) (PLLA). As the PLLA content increased, the melting points of PLC copolymers decreased from 61 to 43 °C. PLC copolymers in vials solubilized at 40–50 °C according to the incorporation of PLLA into the PCL segment. Dexamethasone (Dex)-loaded PLC (MC_xL_y) microspheres were prepared by the oil-in-water (O/W) solvent evaporation/extraction method. The preparation yields were above 70%, and the mean particle size ranged from 30 to 90 μm. The MC_xL_y microspheres also showed controllable melting points in the range of 40–60 °C. Dex-loaded MC_xL_y microspheres showed similar *in vitro* and *in vivo* sustained release patterns after the initial burst of Dex. The *in vitro* and *in vivo* order of the Dex release was $MC_{80}L_{20} > MC_{90}L_{10} > MC_{95}L_5$, which agreed well with the melting point order of the drug carrier. Using *in vivo* fluorescence imaging of fluorescein (FI)-loaded microspheres implanted in animals, we confirmed the sustained release of FI over an extended period. *In vivo* inflammation associated with the PLC microsphere implants was less pronounced than that associated with Poly(lactide-co-glycolide) (PLGA). In conclusion, we successfully demonstrated that it is possible to control Dex release using Dex-loaded MC_xL_y microspheres with different melting points.

Keywords Microsphere · Block copolymer · Melting point · Drug release · Dexamethasone

1 Introduction

Microspheres have been extensively used in drug delivery systems for a variety of drugs, for several years [1–4]. Drug-loaded microspheres possess several attractive features that allow for sustained drug release. In addition, drug-loaded microspheres can be easily administered by simple subcutaneous or intramuscular injection, and these locally injected drug-loaded microsphere depots provide long-term sustained drug release.

Poly(lactide-co-glycolide) (PLGA) is a widely used biodegradable polymer for fabrication of drug-loaded microspheres [5–10]. Several PLGAs with different compositions and molecular weights have been used for many years as drug delivery material.

A common conventional method for the preparation of drug-loaded PLGA microsphere is the oil-in-water emulsion and solvent evaporation technique [11, 12]. Using this technique, the drug is evenly distributed inside a PLGA microsphere. Drug release from the drug-loaded PLGA microsphere is controlled by diffusion, erosion, or a combination thereof. Drug release is also dependent on the composition, molecular weight, and crystallinity of PGLA. In addition, drug release from PLGA is dependent on the polymer degradation rate via hydrolysis, addition of

Ji Hoon Park and Doo Yeon Kwon are equal first authors.

✉ Moon Suk Kim
moonskim@ajou.ac.kr

1 Department of Molecular Science and Technology, Ajou University, 206 Worldcup-ro, Yeongtong-gu, Suwon 16499, Korea

2 Department of Polymer Engineering, Pukyong National University, 365 Sinseon-ro, Nam-gu, Busan 48547, Korea

surfactants to enhance drug diffusion, and an increase in temperature. This increase in temperature enhances polymer mobility via thermal induced structural relaxation of polymer, a well-known phenomenon in polymer science.

Among the several factors that affect drug release from drug-loaded PLGA microspheres, we focused on thermal induced polymer mobility. Some groups have reported that drug diffusion can be controlled by changing the thermal properties of the drug carrier [13, 14]. Meanwhile, thermal induced relaxation of drug carrier can occur not only when polymers approach the melting temperature but also the glass transition temperature [15]. Thus, we examined thermal induced structural relaxation of the drug carrier around the melting temperature. The melting causes polymer chains to gradually relax before the melting point, with the polymer chains completely melted at the melting point [16]. Thus, if structural relaxation of the polymer in the microspheres can occur under body temperature, drug release from the microsphere may be affected.

Poly(L-lactide) (PLLA) is a semicrystalline crystallinity polymer with a melting temperature of approximately 175 °C [17]. Poly(ε-caprolactone) (PCL) is also a semicrystalline polymer and shows a melting point of approximately 60 °C [17].

Generally, the block copolymers prepared from the PLLA and PCL segments can change the crystallinity of block copolymers, suggesting strongly that crystalline aggregation of each segment was interrupted, which induced changes in the melting points of block copolymers [18]. Based on this phenomenon, varying the ratio of PLLA and PCL segments is a convenient way to adjust the melting point.

If we prepare semicrystalline poly(L-lactide-ran-ε-caprolactone) (PLC) copolymers with a melting temperature in the range of 40–60 °C, the block copolymers can exist in the slightly molten state at body temperature. The melting point of PCL is closer to body temperature than that of PLLA. Thus, tailoring the PLLA into the PCL segment can change the melting points of PLC. Consistent with this idea, we previously found that incorporation of the PLLA into the PCL segment decreased melting points by decreasing crystalline aggregation of the PCL segment interrupted by PLLA [19–24].

Thus, the aim of the present study was to prepare PLC copolymers with adjustable melting temperature, strongly considering suitable polymers for inducing thermal relaxation of the drug carrier. To the best of our knowledge, this is the first study to examine the effect of melting points on drug release from microspheres. The present study examined the potential of PLC with melting points in the range of 40–60 °C as a drug carrier. The effect of melting points on the *in vitro* and *in vivo* release profile of dexamethasone

(Dex)-loaded PLC microspheres was investigated. Furthermore, we evaluated the feasibility of developing PLC for Dex release from microspheres.

2 Materials and methods

2.1 Materials

Methoxy poly(ethylene glycol) (MPEG) (number-average molecular weight ($M_n = 750$) and tin octoate ($Sn(Oct)_2$) were used as received from Sigma Aldrich (St. Louis, MO, USA). ε-Caprolactone (CL) was distilled over CaH_2 under reduced pressure. L-Lactide (LA; Boehringer Ingelheim, Blanquefort, France) was recrystallized in ethyl acetate two times. Dex, polyvinyl alcohol (PVA), and fluorescein isothiocyanate (FI) were used as received from Sigma Aldrich (St. Louis, MO, USA).

2.2 Characterization

^{1}H-nuclear magnetic resonance (NMR) spectra were measured using Varian Mercury plus 400 with $CDCl_3$ in the presence of tetramethyl silane (TMS) as an internal standard. Molecular weight distributions of each poly(lactide-ran-ε-caprolactone) (PLC) copolymer were measured by a YL-Clarity GPC system (YL 9170 RI detector) using three columns (Shodex K-802, K-803, and K-804 polystyrene gel columns). GPC was performed by using $CHCl_3$ as an eluent with a flow rate of 1.0 mL/min at 40 °C. To determine the melting temperature (T_m) and heat of fusion (ΔH_m) of PLC copolymers, differential scanning calorimetry (DSC; Q 1000, TA Instruments, Hüllhorst, Germany) was performed from −80 to 100 °C at a heating rate of 5 °C/min under a dry nitrogen atmosphere. X-ray diffraction (XRD; D/MAX-III B, Rigaku, Japan) was used to determine the crystallinity of the PLC copolymers. The radiation of XRD was generated by a Ni filter at 35 kV and 15 mA. The PLC copolymers were placed in a quartz sample holder and scanned from 0° to 60° at a scanning rate of 5°/min. The degree of crystallinity of copolymers was calculated by comparing the ratio of the crystalline peak areas to the total area under the scattering curve.

2.3 Synthesis of PLC (MC_xL_y) copolymers

For preparation of PLC copolymers, all glassware was completely dried by hot heating in a vacuum and then handled under a dry nitrogen atmosphere. The PLC copolymers were assigned as ratios of the PCL and PLLA segment. The typical polymerization procedure of $MC_{90}L_{10}$ (CL/

LA = 90/10) was as follows. The solution of MPEG (0.12 g, 0.16 mmol) and toluene (80 mL) were azeotropically distillated to remove the included water in original MPEG. About toluene of 50 mL was distilled off. CL (4.46 g, 31.0 mmol) and LA (3.54 g, 31.0 mmol) were firstly added and then 0.2 mL of a 0.1 M solution of stannous octoate in dried toluene was added to the MPEG solution under a nitrogen atmosphere at room temperature. After polymerization for 24 h at 130 °C, the reaction solution was poured into a mixture of *n*-hexane and ethyl ether (v/v = 4/1) to precipitate a $MC_{90}L_{10}$. The precipitated polymer was filtered and dried in a vacuum to yield a colorless polymer.

$MC_{95}L_5$ and $MC_{80}L_{20}$ copolymers were prepared is a similar manner. ^{1}H-NMR spectra of the prepared $MC_{95}L_5$, $MC_{90}L_{10}$, and $MC_{80}L_{20}$ copolymers were used to determine the molecular weights and ratios of the PCL and PLLA segments through comparing the total methylene protons in PCL at $\delta = 2.3$ ppm and total methine protons in PLLA at $\delta = 5.2$ ppm with the total methyl protons in MPEG at $\delta = 3.38$ ppm as a standard of 750 g/mol. The prepared MC_xL_y copolymers were added in the vial of 4 mL and incubated at 30, 40, and 50 °C for 2 h. The images of MC_xL_y copolymers were visualized with an optical camera (SX270 HS, Canon, Tokyo, Japan).

2.4 Preparation of Dex-loaded MC_xL_y microspheres

Dex-loaded MC_xL_y microspheres were prepared by the solvent extraction/evaporation technique. MC_xL_y (0.15 g) was dissolved in 0.85 g tetrahydrofuran (THF), and 20 mg Dex was dispersed in the MC_xL_y solution. This solution was then added at a rate of 1 mL/min to 200 mL of 45 °C, 1 wt% aqueous polyvinyl alcohol (PVA) with stirring at 600 rpm. This emulsion was stirred for 2 h at 25 °C. The resulting MC_xL_y microspheres were washed three times with de-ionized water and vacuum dried for 48 h. The prepared MC_xL_y microspheres were added in the vial of 4 mL and incubated at 25, 37, 45, and 50 °C for 2 h. The images of MC_xL_y microspheres were visualized by using an optical camera (Canon, SX270 HS).

2.5 Characterization of MC_xL_y microspheres

The encapsulation efficiency of Dex-loaded MC_xL_y microspheres and the release amounts from each Dex-loaded MC_xL_y microsphere was determined using a high performance liquid chromatography (HPLC) system (1200 series in Agilent Technologies, Waldbronn, Germany) with a Sunfire C18 column (4.6 × 150 mm, 5 mm) and an ultraviolet (UV) absorbance detector set at 242 nm. Three independent encapsulation efficiencies and release amounts for each Dex-loaded MC_xL_y microsphere preparation were determined by using eluent of acetonitrile/water (50/50

v/v) at a flow rate of 1.0 mL/min. The weight for encapsulation efficiency and the release amounts was calculated by comparison to standard calibration curves prepared with known weight-concentrations of Dex.

Three independent particle size of each Dex-loaded MC_xL_y microsphere was determined by dynamic light scattering (ELSZ-1000; Otsuka Electronics, Osaka, Japan) at room temperature and determined by following the manufacturer's protocol.

2.6 *In vitro* Dex release

Approximately 20 mg of Dex-loaded MC_xL_y microspheres were dispersed in 5 mL phosphate-buffered saline (PBS). For Dex release experiments, the dispersed solutions were incubated at 37 °C and shaken at 100 rpm. 1 mL Dex released solution was collected at pre-determined times and replaced with same amount of fresh media within interval of 10 s. The collected solutions were analyzed using HPLC (as described in Sect. 2.5). The released Dex amount at each time interval was calculated by comparing with a standard calibration curve prepared from known Dex concentrations in PBS. Three independent release experiment was performed and the results were presented as mean ± standard deviation (SD). The results were analyzed using one-way analysis of variance (ANOVA) with Bonferroni's post hoc test and SPSS 12.0 software (SPSS Inc., Chicago, IL, USA).

2.7 *In vivo* fluorescence imaging

To monitor real-time *in vivo* release in live animals, FI-loaded $MC_{90}L_{10}$ microsphere solution (10 mg microsphere with a 20% w/v solution of 5% D-mannitol, 2% carboxymethylcellulose, and 0.1% Tween 80 as an injection vehicle) was prepared, and 250 μL of the solution was subcutaneously injected into the left dorsum of a 6-week-old male nude mouse using a 21-gauge needle. For 5 weeks, side-view images of the mice were visualized at a wavelength of 515 nm (excitation wavelength, 470 nm) of a fluorescence imaging system (FO ILLUM PL-800; Edmund Optics, Barrington, NJ, USA) with 150 W EKE Quartz Halogen light and glass reference number OG515 filter. Each fluorescence image was digitized by using a charge-coupled device and then visualized using Axiovision Rel. 4.8 software. The intensity of each fluorescence image was determined using ImageJ version 1.47 (National Institutes of Health, Bethesda, MD, USA).

2.8 *In vivo* Dex release

Sixteen Sprague–Dawley (SD) rats (280–300 g, 6 weeks, male) were used to determine the Dex release amounts

from Dex-loaded MC_xL_y microspheres. All animals were treated in accordance with the guidelines of the Institutional Animal Experiment Committee at Ajou University School of Medicine (Approval No. 2016-0048). Dex-loaded MC_xL_y microspheres were sterilized using an UV ray overnight. The rats were separated into eight experiment groups at 1, 3, 5, 10, 14, 21, and 28 days. Each rat was anesthetized using zoletile and rompun (1:1 ratio, 1.5 mL kg^{-1}). Dex-loaded MC_xL_y microsphere solution was composed of 10 mg microsphere, a 20% w/v solution of 5% D-mannitol, 2% carboxymethylcellulose and 0.1% Tween 80 as an injection solution. The 250 μL solution was individually injected subcutaneously under the dorsal skin. The rats were sacrified 1, 3, 5, 10, 14, 21, and 28 days after the injection. The Dex-loaded MC_xL_y microspheres were removed individually from the subcutaneous dorsum. The Dex amount in each microsphere was analyzed using HPLC, as described in Sect. 2.5. The release amounts of Dex were determined by comparing Dex concentrations between the initial injected Dex-loaded MC_xL_y microsphere and the remainder of Dex-loaded MC_xL_y microsphere at each time point. Each release experimental group was individually performed for three rats and the results were presented as mean ± standard deviation (SD). The results were analyzed using one-way analysis of variance (ANOVA) with Bonferroni's post hoc test and SPSS 12.0 software (SPSS Inc., Chicago, IL, USA).

2.9 *In vivo* scanning electron microscope (SEM) observation

The morphology of the *in vivo* microspheres was observed by SEM (Stereoscan 440; Leica, Wetzlar, Germany). The microspheres were removed from the rat at 2 and 4 weeks. The removed *in vivo* microspheres were rapidly immersed in a liquid nitrogen bath to prevent structural changes of the MC_xL_y microsphere, and then freeze-dried at a freeze dryer of −75 °C. Each dried MC_xL_y microsphere was coated with a thin layer of gold in an argon atmosphere using a plasma-sputtering apparatus (Ted Pella, Cressington 108 Auto, Redding, CA, USA) and then examined by SEM.

2.10 Histological analysis

Dex-loaded $MC_{90}L_{10}$ microsphere implanted rats were sacrificed at 1, 2 and 4 weeks. The Dex-microsphere implants were immediately harvested from subcutaneous dorsum, immediately fixed with 10% formalin. The paraffin wax embedded specimens were sectioned at 4 μm thickness along the longitudinal axis of the implant. Each section was stained with hematoxylin and eosin (H&E) and examined by light microscopy.

Each slide was firstly rinsed with 0.05% Tween 20 solution in PBS (PBS-T) for 6-diamino-2-phenylindole dihydrochloride (DAPI; Sigma-Aldrich, St Louis, MO, USA) and ED1 staining. The slides were subsequently blocked with solution of 5% bovine serum albumin (BSA; Bovogen, Keilor East, Australia) and 5% horse serum (HS; Gibco, Invitrogen, Carlsbad, CA, USA) in PBS for 1 h at 37 °C. The slides were exposed to mouse anti-rat CD68 antibody (ED1; Serotec, Oxford, UK) and then incubated for 15 h at 4 °C. The slides was rinsed with PBS-T and then incubated with the secondary antibody (goat anti-mouse Alexa Fluor 594; Invitrogen) for 3 h in the dark at room temperature. The slides were washed with PBS-T and counterstained with DAPI, and then developed by fluorescent mounting solution (DAKO, Carpinteria, CA, USA). Immunofluorescent images were visualized with an Axio Imager A1 (Carl Zeiss Microimaging GmbH, Göttingen, Germany) equipped with Axiovision Rel. 4.8 software (Carl Zeiss).

3 Results and discussion

3.1 Preparation of MC_xL_y copolymers

The melting points depended mainly on the compositions of PCL and PLLA. Previously, we demonstrated that the melting points of MC_xL_y copolymers could be controlled by varying the compositions of PCL and PLLA [19]. The aim of the current study was to compare MC_xL_y copolymers with different melting points as a drug carrier. MC_xL_y copolymers were prepared with varying compositions of PCL and PLLA.

Table 1 summarizes the results obtained for the different MC_xL_y copolymers. Colorless copolymers greater than 90% yield after precipitation. The featuring peaks of PCL, PLLA, and MPEG were observed in the ^{1}H-NMR spectrum of $MC_{90}L_{10}$ copolymer, as shown in Fig. 1.

The ratios of the PCL and PLLA segments in the MC_xL_y copolymers were determined by measuring the intensities of the total methoxy protons *1* and methylene protons *2* of MPEG against the methylene protons 2.3 and 5.1 ppm of PCL and PLLA in ^{1}H-NMR spectra, respectively. CL and LA monomers were randomly incorporated to produce MC_xL_y copolymers in agreement with the changes in the feed ratio. The molecular weights of PCL and PLLA, determined by ^{1}H-NMR, also were in accordance with those calculated from the designed ratio of the CL and LA monomer to MPEG. Thus, the MC_xL_y copolymer was prepared successfully as a drug carrier for the following experiments.

3.2 Characterization of MC_xL_y copolymers

If segments in block copolymers have crystalline polymer, the block copolymers have crystallinity and/or melting

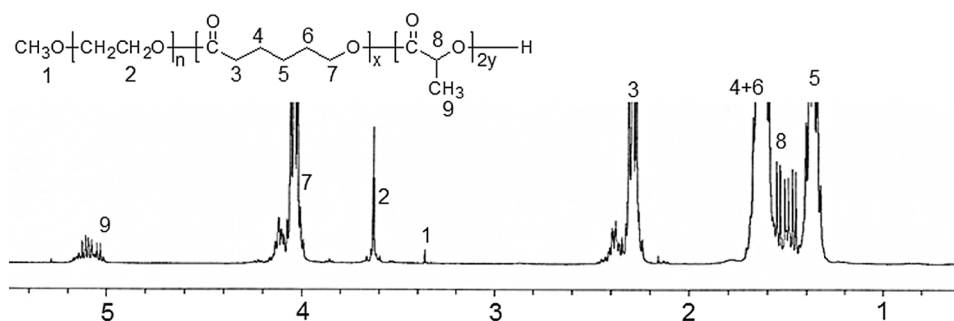**Table 1** Synthesis of MC_xL_y copolymers

No.	$[M]_{ratio}$ (CL/LA)	Yield (%)	M_n^a	M_w/M_n^b	T_m (°C)^c	ΔH (J/g)^c	X_c^d
$MC_{100}L_0$	100/0	95	750–20,300	1.24	61	92.1	41.0
$MC_{95}L_5$	94/6	94	750–17,000	1.38	53	62	36.8
$MC_{90}L_{10}$	90/10	91	750–20,100	1.42	50	53	27.0
$MC_{80}L_{20}$	79/21	92	750–19,000	1.45	44	24.7	24.4
$MC_{70}L_{30}$	70/30	86	750–20,100	1.32	43	0.5	7.5

[a] Determined by ^{1}H-nuclear magnetic resonance (NMR)

[b] Measured by GPC (based on standard polystyrene)

[c] Measured by differential scanning calorimetry (DSC)

[d] Determined by X-ray diffraction

Fig. 1 ^{1}H-nuclear magnetic resonance (NMR) spectrum of $MC_{90}L_{10}$ copolymer

points, and their crystallinities depend mainly on the composition of the polymer segments. Therefore, the melting points, enthalpies, and crystallinities of MC_xL_y copolymers were measured by DSC and XRD (Table 1).

Generally, PCL and PLLA have melting points of ~ 60 and ~ 175 °C, respectively. However, one exothermic peak was observed at approximately 43–61 °C by DSC of MC_xL_y copolymers. There was no exothermic peak in the range of ~ 175 °C at the melting of the crystal phase of the PLLA segment. These data demonstrate the phase compatibility of the PCL and PLLA block segment, even though the PCL and PLLA segments were covalently coupled.

The $MC_{100}L_0$ copolymer showed 92 J/g of enthalpy at 61 °C, assignable to the crystallization of the PCL segment. The degree of crystallinity for the $MC_{100}L_0$ copolymer was estimated to be 41% from XRD. As the PLLA contents increased, the melting points and the enthalpy of MC_xL_y copolymers decreased from 61 to 43 °C, and the degree of crystallinity decreased from 41 to 7.5%.

Next, we examined the melting of the MC_xL_y copolymers in the vial based on changes in temperature (Fig. 2). $MC_{100}L_0$ copolymer did not melt at temperatures up to 50 °C. $MC_{95}L_5$ and $MC_{90}L_{10}$ copolymers showed no melting at 30 and 40 °C but were slightly melted at 50 °C. $MC_{80}L_{20}$ copolymer showed slightly melted copolymer at 30 and 40 °C but was completely melted at 50 °C. Furthermore, the $MC_{70}L_{30}$ copolymer was completely melted even at 30 °C. These findings support the idea that the MC_xL_y copolymers prepared in this work had controllable melting points.

We chose $MC_{95}L_5$, $MC_{90}L_{10}$, and $MC_{80}L_{20}$ copolymers, which were soluble in the suitable temperature range of 40–50 °C, as drug carrier in the following experiments, because $MC_{100}L_0$ and $MC_{70}L_{30}$ copolymers did not solubilize and were completely solubilized, respectively, at temperatures approximately 40 °C.

3.3 Preparation of Dex-loaded MC_xL_y microspheres

Figure 3A shows a schematic representation of the preparation of Dex-loaded MC_xL_y microspheres. Dex-loaded MC_xL_y microspheres were prepared by the O/W solvent evaporation/extraction method. Both MC_xL_y and Dex were dissolved in a volatile THF organic solvent, and the resulting organic phase was emulsified at 45 °C under mechanical stirring in a continuous aqueous phase that contained a PVA emulsifier. MC_xL_y microspheres were prepared as a result of solvent extraction and evaporation.

Images of the prepared spherical microspheres with a smooth surface structure are shown in Fig. 3B. Table 2 summarizes the yield, diameter, and encapsulation for the Dex-loaded MC_xL_y microspheres obtained. The preparation yields of $MC_{95}L_5$, $MC_{90}L_{10}$, and $MC_{80}L_{20}$ were 82, 79 and 73%, respectively. Their mean particle sizes were 91, 87, and 63 μm, respectively. The yields and mean particle sizes slightly decreased as the melting points decreased. FI-loaded $MC_{90}L_{10}$ microspheres were greenish in color due to the green color of FI (Fig. 3B3, B4).
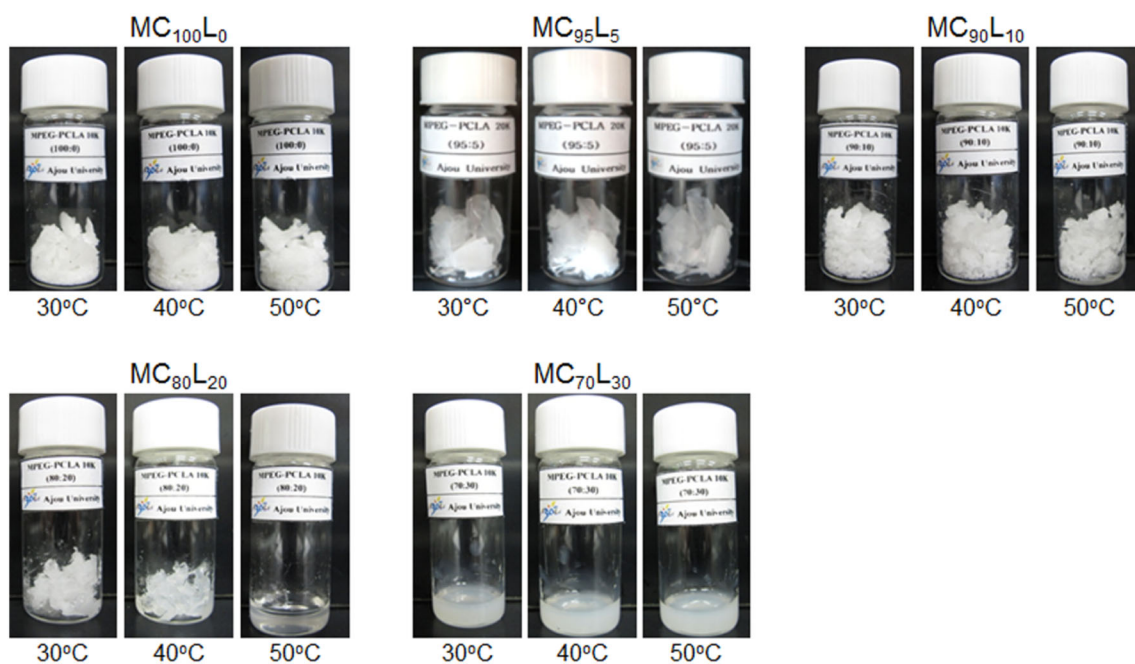
Fig. 2 Optical images of $MC_{100}L_0$, $MC_{95}L_5$, $MC_{90}L_{10}$, $MC_{80}L_{20}$, and $MC_{70}L_{30}$ copolymers at different temperatures
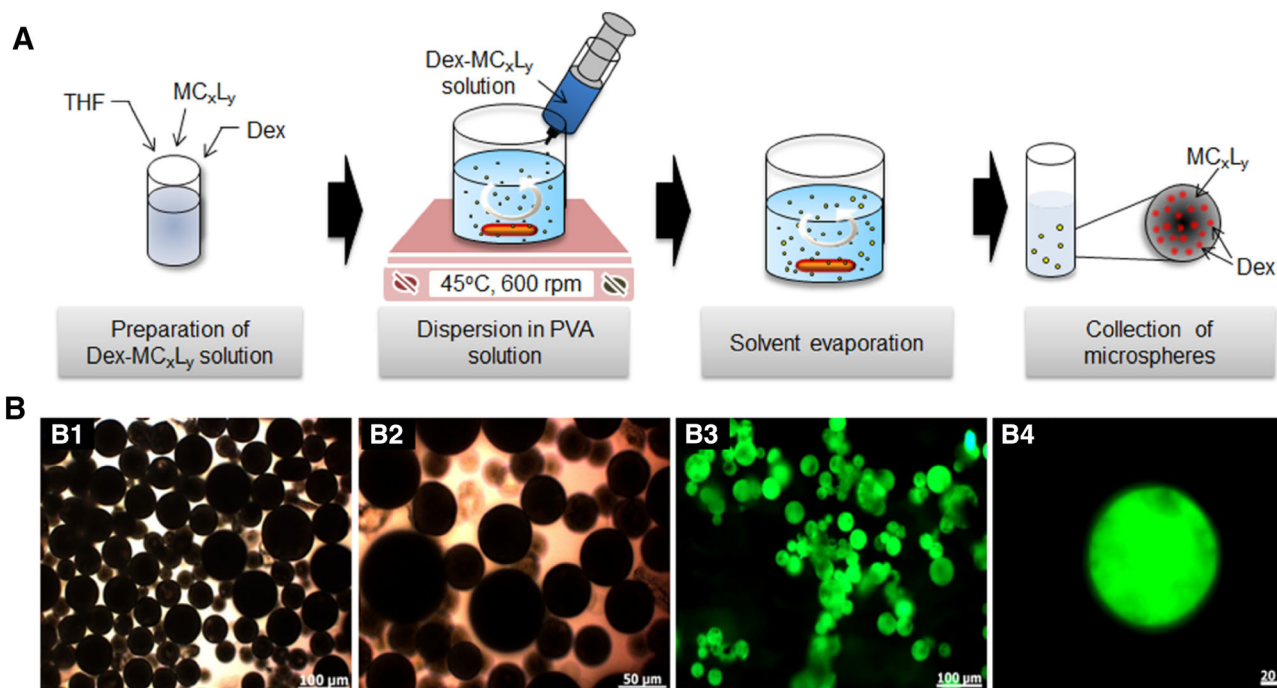

Fig. 3 A Schematic representation for the manufacturing of Dex-loaded MC_xL_y microspheres, **B1**, **B2** microscopic image of Dex-loaded $MC_{90}L_{10}$ microspheres, **B1** ×100 (*scale bar* indicates 100 μm) and **B2** ×200 (*scale bar* indicates 50 μm), and **B3**, **B4** fluorescence image of fluorescein (FI)-loaded $MC_{90}L_{10}$ microspheres, **B3** ×100 (*scale bar* indicates 100 μm) and **B4** ×400 (*scale bar* indicates 20 μm)

3.4 Thermal characterization of MC_xL_y microspheres

It is conceivable that the prepared MC_xL_y microspheres could be affected by the melting points, enthalpies, and crystallinities of MC_xL_y copolymers. As described in previous Sect. 3.3, MC_xL_y microspheres were prepared using MC_xL_y copolymers with different melting points.

The MC_xL_y microspheres in the vial were examined by changing the temperature from 25 to 50 °C, as shown in

Table 2 Characterization of Dex-loaded MC_xL_y microspheres

No.	Yield (%)[a]	Diameter (μm)	Encapsulation efficiency (%)[b]
$MC_{95}L_5$	82	91 ± 22	62
$MC_{90}L_{10}$	79	87 ± 18	58
$MC_{80}L_{20}$	73	63 ± 21	41

[a] Weight of microsphere/weight of the feeding copolymer and Dex $\times$ 100

[b] Weight of the Dex loaded in microsphere/weight of the feeding Dex $\times$ 100 (The weight of Dex was calculated by comparison to standard calibration curves prepared with known weight-concentrations of Dex)
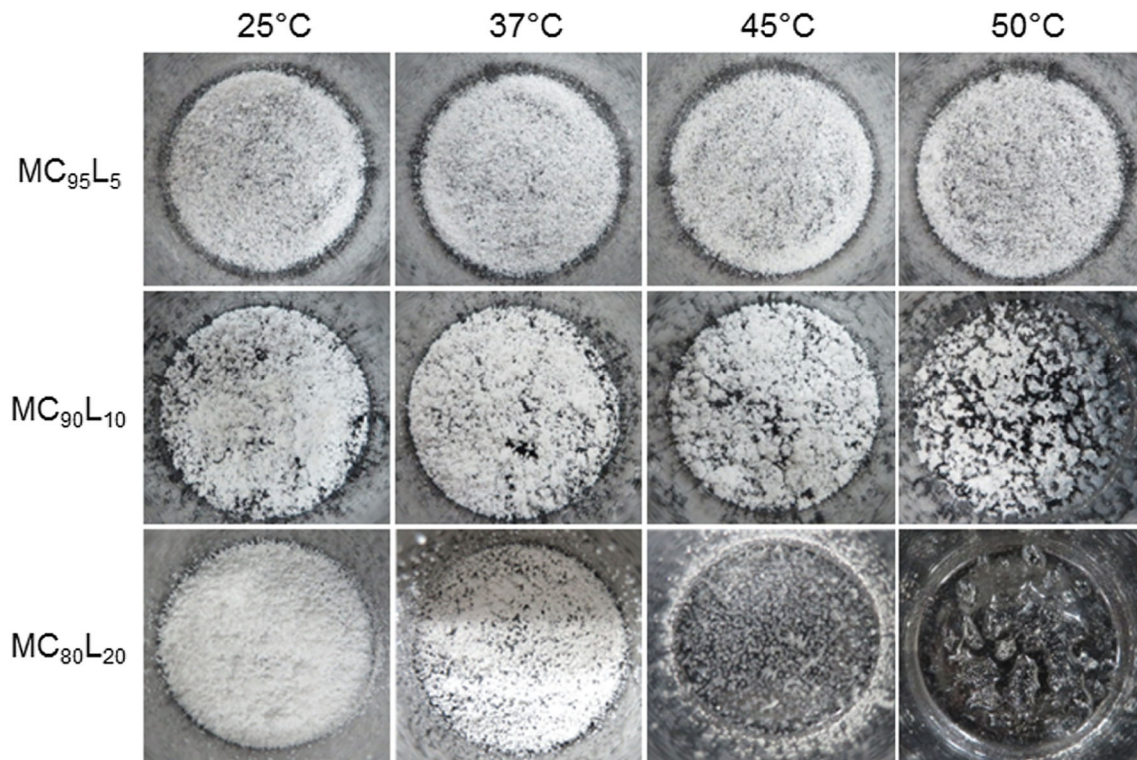

Fig. 4 Images of Dex-loaded $MC_{95}L_5$, $MC_{90}L_{10}$, and $MC_{80}L_{20}$ microspheres at 25–50 °C

Fig. 4. $MC_{95}L_5$ showed slightly aggregated microspheres due to the slight melting of the microspheres at 50 °C, but the shape of the microspheres was maintained at temperatures below 45 °C. On imaging, $MC_{90}L_{10}$ and $MC_{80}L_{20}$ showed aggregated microspheres due to melting at 45 °C. This finding demonstrated that the MC_xL_y microspheres prepared in this work had controllable melting points.

3.5 *In vitro* and *in vivo* Dex release from Dex-loaded MC_xL_y microspheres

The aim of this study was to examine Dex release performance of Dex-loaded MC_xL_y microspheres. First, to evaluate *in vitro* Dex release, Dex-loaded MC_xL_y microspheres were incubated in PBS at 37 °C for 18 days. Figure 5A shows the *in vitro* Dex release plots for the cumulative released amounts versus time. The cumulative *in vitro* Dex release from Dex-loaded MC_xL_y microspheres was approximately 32, 42, and 52% for $MC_{95}L_5$, $MC_{90}L_{10}$, and $MC_{80}L_{20}$, respectively, at 1 day, implying an initial burst of Dex. Subsequently, Dex release was maintained at almost the same level for up to 18 days, indicating sustained release of Dex. The amount of released Dex for $MC_{80}L_{20}$ was higher than that of $MC_{90}L_{10}$ and that of $MC_{95}L_5$.

Next, Dex-loaded MC_xL_y microspheres were implanted into SD rats and allowed to develop for 28 days. *In vivo* Dex release was determined by the remainder of Dex amount inside Dex-loaded MC_xL_y microspheres removed at pre-determined times.

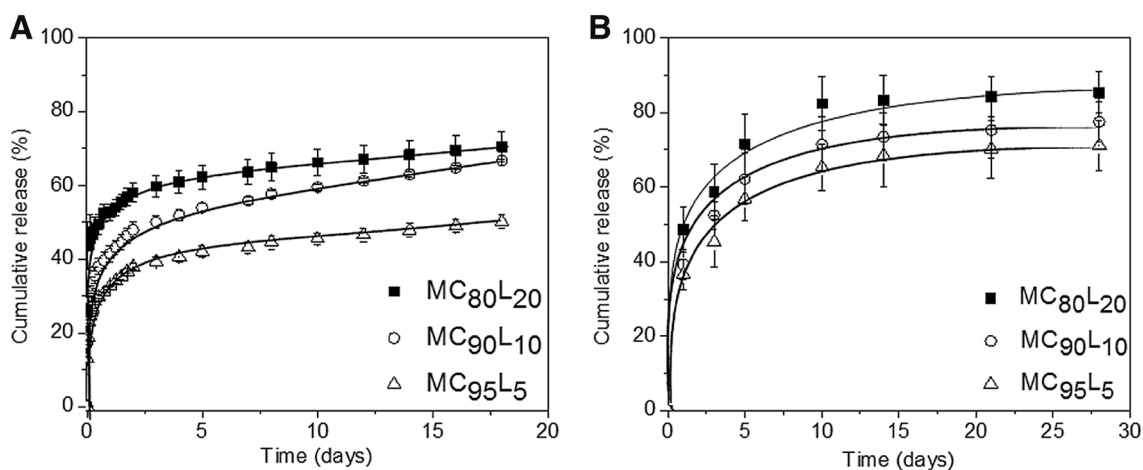Figure 5B shows the plots for *in vivo* cumulative release of Dex from Dex-loaded MC_xL_y microspheres. The amount

Fig. 5 Accumulated release of Dex from Dex-loaded MC95L5, MC90L10, and MC80L20 microspheres **A** *in vitro* for 18 days and **B** *in vivo* for 21 days
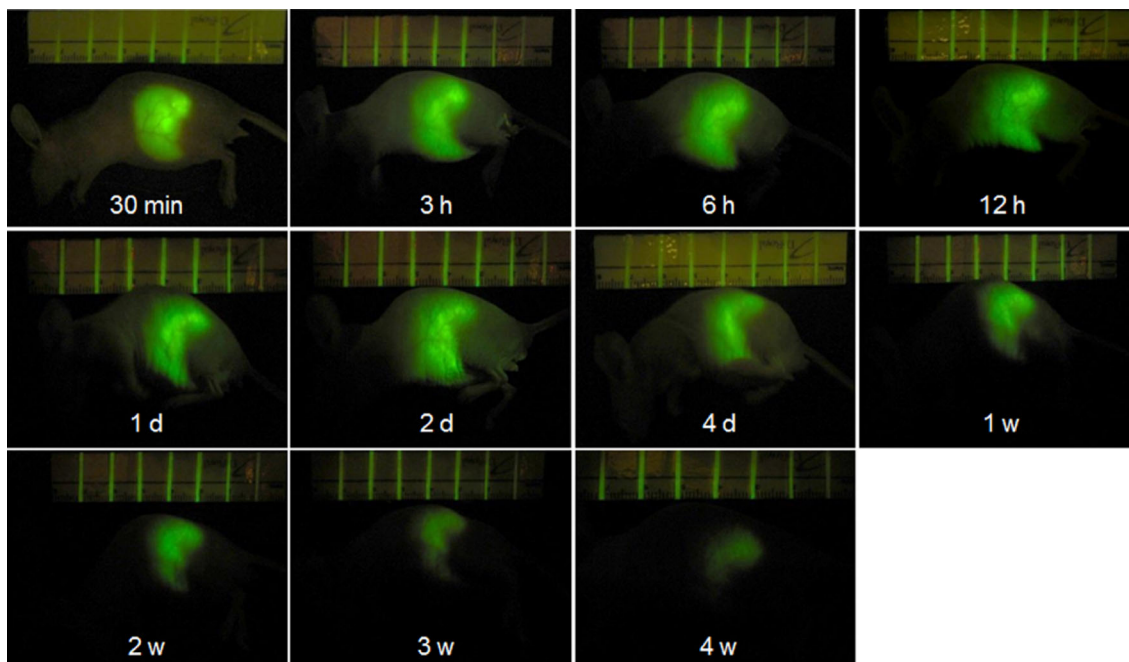

Fig. 6 *In vivo* fluorescence image of a nude mouse injected with FI-loaded $MC_{90}L_{10}$ microsphere for 4 weeks after injection

of Dex released from Dex-loaded MC_xL_y microspheres at 1 day was 37, 39, and 49% for $MC_{95}L_5$, $MC_{90}L_{10}$, and $MC_{80}L_{20}$, respectively. After the initial burst release, the amount of Dex released was almost the same, regardless of the copolymers used.

The *in vitro* and *in vivo* order of Dex release was $MC_{80}L_{20} > MC_{90}L_{10} > MC_{95}L_5$, which was consistent with the melting point order of the drug carrier. The *in vitro* and *in vivo* releasing patterns of Dex from Dex-loaded MC_xL_y microspheres were similar. This finding implies that Dex release from Dex-loaded MC_xL_y microspheres could be controlled by adjusting the melting point of the

drug carrier. In summary, we successfully confirmed the possibility of controlling Dex release by using Dex-loaded MC_xL_y microspheres with different melting points.

Real time fluorescence imaging was used to investigate *in vivo* sustained release of FI as a model drug from FI-loaded $MC_{90}L_{10}$ microspheres in live animals. Fluorescence images were acquired from a nude mouse after subcutaneous implantation of FI-loaded $MC_{90}L_{10}$ microspheres (Fig. 6). Green fluorescence was observed immediately at the injected site after implantation, with diffusion of FI. The area of fluorescence gradually increased and maximized at 12 h after administration, probably implying
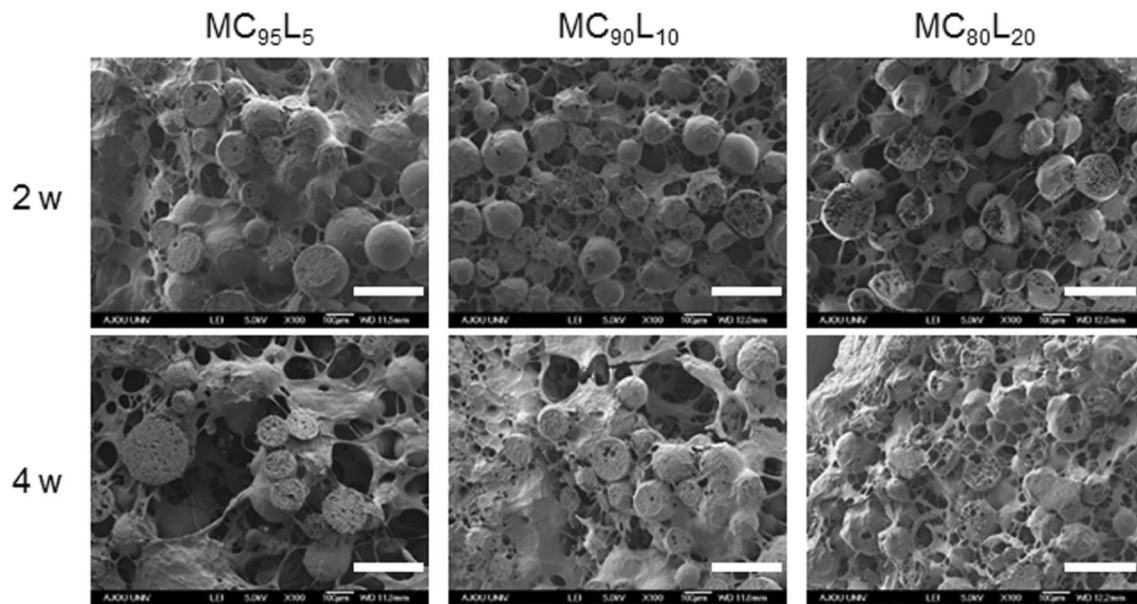
Fig. 7 Scanning electron microscope (SEM) images of Dex-loaded $MC_{95}L_5$, $MC_{90}L_{10}$, and $MC_{80}L_{20}$ microspheres 2 and 4 weeks after injection (*scale bar* indicates 200 μm)
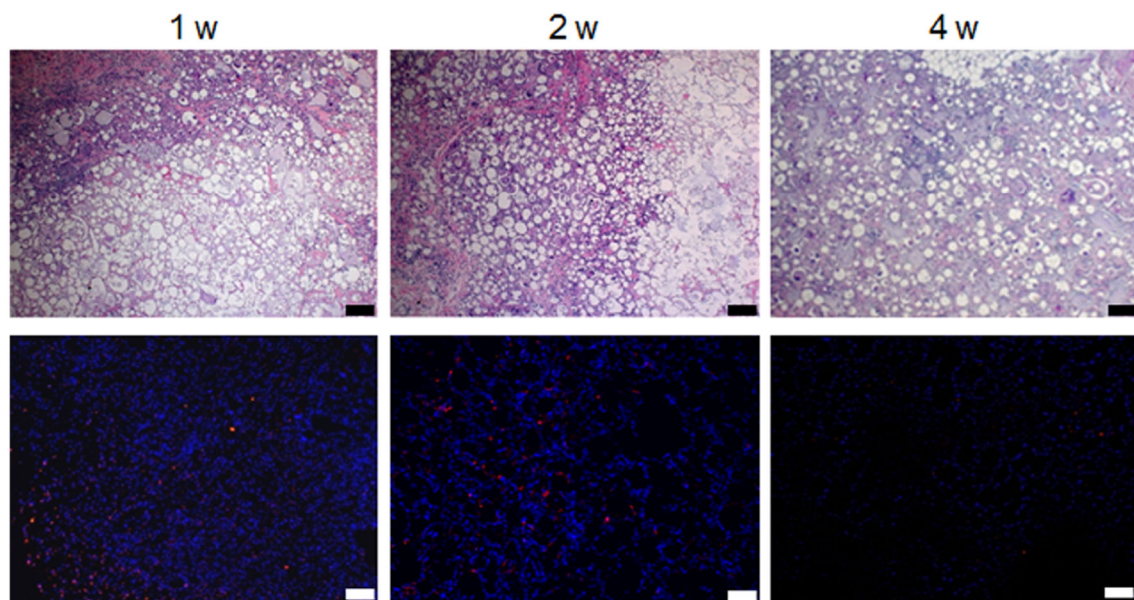

Fig. 8 Hematoxylin and eosin (H&E) and CD68 antibody (ED1) immunohistochemical staining of Dex-loaded $MC_{90}L_{10}$ microspheres 1, 2, and 4 weeks after injection (the *scale bars* represent 200 μm for H&E and 100 μm for ED1)

the *in vivo* burst effect. At 4 days, the area of fluorescence reached at similar fluorescence with initially injected microsphere. Even though from 4 days the fluorescence images showed the gradually decreased intensity and area, they were still observed up to 28 days, indicating sustained release of FI. The remaining FI was still detectable from the removed microspheres even at 35 days.

We found that Dex was released *in vitro* and *in vivo* from microspheres by two-phase kinetics: a fast initial burst on the first day, followed by a sustain release for up to 18 or 28 days. Some Dex was remained inside the microspheres. The remained Dex within the microspheres after *in vitro* and *in vivo* release for 18 or 28 days were probably due to the incomplete biodegradation of microspheres, because we already reported 30–40% biodegradation of PLC with similar concentration even at 8 weeks [19, 25]. Thus, we conjecture that the remained Dex can be completely release through biodegradation by

in vitro and *in vivo* biological media after longer release period.

3.6 SEM morphology of *in vivo* Dex-loaded MC_xL_y microspheres

To examine the *in vivo* morphology of Dex-loaded MC_xL_y microspheres with different melting points, Dex-loaded MC_xL_y microspheres removed from rats after 2 and 4 weeks after implantation were frozen in liquid nitrogen, freeze-dried, and observed by SEM (Fig. 7).

Most Dex-loaded MC_xL_y microspheres remained round in shape in SEM images. However, Dex-loaded $MC_{80}L_{20}$ microspheres exhibited a more crushed spherical structure than those of Dex-loaded $MC_{95}L_5$ and $MC_{90}L_{10}$ microspheres at 2 and 4 weeks. Cross-sectioned microspheres showed pore structure, likely indicating the structure formed by released Dex. The pore structure of Dex-loaded $MC_{80}L_{20}$ microspheres appeared higher than those of Dex-loaded $MC_{95}L_5$ and $MC_{90}L_{10}$ microspheres at 2 and 4 weeks, implying greater release of Dex.

3.7 Histology examination of *in vivo* Dex-loaded MC_xL_y microspheres

To assess the *in vivo* histology of Dex-loaded $MC_{90}L_{10}$ microspheres, the tissues into which a microsphere implant had been transplanted were examined by H&E and CD68 antibody (ED1) staining (Fig. 8).

H&E-stained histological sections of harvested microsphere implants revealed tissue integrity after 1, 2, and 4 weeks. The Dex-loaded $MC_{90}L_{10}$ microsphere exhibited large microspheres even at 4 weeks. The number of macrophages and neutrophils was increased in the border zone of the microspheres and host tissue.

The ED1 antibody is a macrophage marker and is considered a unique *in vivo* indicator of the inflammatory response. Tissues were stained with ED1 antibody (red) to determine inflammatory cell accumulation and with DAPI (blue) to confirm the extent of host cell infiltration within and near the transplanted microsphere.

As shown by DAPI staining, many host cells surrounded the microsphere. In addition, ED1-positive cells were found at the surface and in tissues surrounding the microsphere, indicating macrophage accumulation. ED1-positive cells were counted and normalized to the stained tissue area. The number of ED1-positive cells in all formulations was 25, 34, and 17% for 1, 2, and 4 weeks, respectively. In this study, the inflammation within Dex-loaded $MC_{90}L_{10}$ microsphere was significantly lower than that observed in response to PLGA microspheres [26, 27].

Collectively, in this work we examined the effect of melting points on drug release from microspheres. We successfully prepared PLC copolymers with different melting points as a drug carrier for microspheres and demonstrated that the release of Dex from the MC_xL_y microspheres was correlated with the melting order of the drug carrier in the microspheres. In addition, we demonstrated the feasibility of developing PLC for controlled release of Dex from microspheres.

Compliance with ethical standards

Conflict of interest The authors declare that they have no conflict of interest.

Ethical statement This study was conducted under the approval of the Institutional Animal Experiment Committee at Ajou University School of Medicine (Approval No. 2016-0048).

References

1. Andhariya JV, Burgess DJ. Recent advances in testing of microsphere drug delivery systems. Expert Opin Drug Deliv. 2016;13:593–608.
2. Ramazani F, Chen W, van Nostrum CF, Storm G, Kiessling F, Lammers T, et al. Strategies for encapsulation of small hydrophilic and amphiphilic drugs in PLGA microspheres: state-of-the-art and challenges. Int J Pharm. 2016;29:358–67.
3. Sellers DL, Kim TH, Mount CW, Pun SH, Horner PJ. Poly(lactic-co-glycolic) acid microspheres encapsulated in Pluronic F-127 prolong hirudin delivery and improve functional recovery from a demyelination lesion. Biomaterials. 2014;35:8895–902.
4. Song W, Liu G, Li J, Luo Y. Bone morphogenetic protein-2 sustained delivery by hydrogels with microspheres repairs rabbit mandibular defects. Tissue Eng Regen Med. 2016;13:750–61.
5. Tomic I, Vidis-Millward A, Mueller-Zsigmondy M, Cardot JM. Setting accelerated dissolution test for PLGA microspheres containing peptide, investigation of critical parameters affecting drug release rate and mechanism. Int J Pharm. 2016;30:42–51.
6. Ko Y, Park JH, Lee JB, Oh HH, Park WH, Cho D, et al. Growth behavior of endothelial cells according to electrospun poly(D,L-Lactic-Co-Glycolic Acid) fiber diameter as a tissue engineering scaffold. Tissue Eng Regen Med. 2016;13:343–51.
7. de Alteriis R, Vecchione R, Attanasio C, De Gregorio M, Porzio M, Battista E, et al. A method to tune the shape of protein-encapsulated polymeric microspheres. Sci Rep. 2015;30:12634.
8. Bae YJ, Cho CH, Lee WJ, Huh JS, Lim JO. Optimization of recombinant human platelet-derived growth factor-BB encapsulated in Poly (Lactic-co-Glycolic Acid) microspheres for applications in wound healing. Tissue Eng Regen Med. 2016;13:13–20.
9. Park JS, Park KH. Light enhanced bone regeneration in an athymic nude mouse implanted with mesenchymal stem cells embedded in PLGA microspheres. Biomater Res. 2016;20:4.
10. Shen J, Lee K, Choi S, Qu W, Wang Y, Burgess DJ. A reproducible accelerated *in vitro* release testing method for PLGA microspheres. Int J Pharm. 2016;498:274–82.
11. Ma G. Microencapsulation of protein drugs for drug delivery: strategy, preparation, and applications. J Control Release. 2014;10-324-340.

12. Crotts G, Park TG. Protein delivery from poly(lactic-co-glycolic acid) biodegradable microspheres: release kinetics and stability issues. J Microencapsul. 1988;15:699–713.

13. Rawat A, Burgess DJ. Effect of physical ageing on the performance of dexamethasone loaded PLGA microspheres. Int J Pharm. 2011;415:164–8.

14. Allison SD. Effect of structural relaxation on the preparation and drug release behavior of poly(lactic-co-glycolic)acid microparticle drug delivery systems. J Pharm Sci. 2008;97:2022–35.

15. Liu J, Rigsbee DR, Stotz C, Pikal MJ. Dynamics of pharmaceutical amorphous solids: the study of enthalpy relaxation by isothermal microcalorimetry. J Pharm Sci. 2002;91:1853–62.

16. Hia IL, Vahedi V, Pasbakhsh P. Self-healing polymer composites: prospects, challenges, and applications. Polym Rev. 2016;56:225–61.

17. Pereira H, Correlo VM, Silva-Correia J, Oliveira JM, Reis RL, Espregueira-Mendes J. Migration of "bioabsorbable" screws in ACL repair. how much do we know? A systematic review. Knee Surg Sports Traumatol Arthrosc. 2013;21:986–94.

18. Rachmawati R, Woortman AJ, Kumar K, Loos K. Inclusion complexes between polytetrahydrofuran-b-amylose block copolymers and polytetrahydrofuran chains. Macromol Biosci. 2015;15:812–28.

19. Park JH, Kang HJ, Kwon DY, Lee BK, Lee BL, Jang JW, et al. Biodegradable poly(lactide-co-glycolide-co-ε-caprolactone) block copolymers—evaluation as drug carriers for a localized and sustained delivery system. J Mater Chem B. 2015;3:8143–53.

20. Lee JW, Lee HY, Park SH, Park JH, Kim JH, Min BH, et al. Preparation and evaluation of dexamethasone-loaded electrospun nanofiber sheets as a sustained drug delivery system. Materials (Basel). 2016;9:E175.

21. Kwon DY, Kwon JS, Park SH, Park JH, Jang SH, Yin XY, et al. A computer-designed scaffold for bone regeneration within cranial defect using human dental pulp stem cells. Sci Rep. 2015;5:12721.

22. Kwon DY, Tai GZ, Park JH, Lee BK, Lee JH, Kim JH, et al. Preparation of methoxy poly(ethyleneglycol)-b-poly(ε-caprolactone-co-L-lactide) and characterization as biodegradable micelles. J Polym Res. 2014;21:474.

23. Kim JI, Kim DY, Kwon DY, Kang HJ, Kim JH, Min BH, et al. An injectable biodegradable temperature-responsive gel with an adjustable persistence window. Biomaterials. 2012;33:2823–34.

24. Kang YM, Lee SH, Lee JY, Son JS, Kim BS, Lee B, et al. A biodegradable, injectable, gel system based on MPEG-b-(PCL-ran-PLLA) diblock copolymers with an adjustable therapeutic window. Biomaterials. 2010;31:2453–60.

25. Park JH, Lee BK, Park SH, Kim MG, Lee JW, Lee HY, et al. Preparation of biodegradable and elastic poly(ε-caprolactone-co-lactide) copolymers and evaluation as a localized and sustained drug delivery carrier. Int J Mol Sci. 2017;18:E671.

26. Kim BS, Oh JM, Hyun H, Kim KS, Lee SH, Kim YH, et al. Insulin-loaded microcapsules for in vivo delivery. Mol Pharm. 2009;6:353–65.

27. Kim BS, Oh JM, Seo KS, Cho JS, Kim KS, Lee B, et al. BSA-FITC-loaded microcapsules for in vivo delivery. Biomaterials. 2009;30:902–9.